Int. J. Heat Mass Transfer. Vol. 33, No. 5, pp. 953–963, 1990
Printed in Great Britain

0017–9310/90 $3.00 + 0.00
© 1990 Pergamon Press plc

Convective heat transfer inhibition in an annular porous layer rotating at weak angular velocity

L. ROBILLARD† and K. E. TORRANCE
Sibley School of Mechanical and Aerospace Engineering, Cornell University, Ithaca, NY 14853, U.S.A.

(*Received* 24 *June* 1988 *and in final form* 3 *August* 1989)

Abstract—A study is made of natural convection in a horizontal annular porous layer in rotation about its axis. Isothermal boundary conditions are applied on both inner and outer boundaries, with the outer boundary being warmer. For such conditions, no symmetry with respect to a vertical diameter can be expected for the flow and temperature fields and the whole annular region must be considered. Two-dimensional steady state solutions are obtained numerically. Results indicate that the rotation generates a net circulating flow around the annulus relative to the porous matrix and drastically reduces the overall heat transfer. These effects occur at relatively low angular velocities for which the centrifugal forces are negligible compared to gravity, and inertial effects may be neglected.

1. INTRODUCTION

FREE CONVECTION in containers rotating about a horizontal axis arises in food industries where thermal processing of contained fluids is done for pasteurization and sterilization. In many thermal processing systems, the cans, while being maintained horizontal, are entrained into complex motions, a basic feature of which is rotation about their axes [1–3]. Since the processing time is related to the heat transfer across the can surface, it is important to know how the rotation affects the heat transfer. The present study pertains to that goal.

Within the context of convective heat transfer, we want to examine the interaction between rotation about a horizontal axis and the gravity force. For simplicity, we consider a horizontal annulus rotating about its axis and filled with a fluid-saturated porous medium. Uniform temperatures are imposed on the inner and outer boundaries of the annulus, with the outer boundary being the warmer boundary. The flow in the annulus is assumed to be two-dimensional in a vertical, r–θ plane; the rotational rate of the annulus is taken as constant. The foregoing is, of course, a considerable simplification of the food processing problem. However, the annulus, with differentially heated walls, admits steady flow solutions which are not possible in a cylinder subjected to a step change of wall temperature. The present study provides numerical solutions for the flow in a fluid-saturated porous annulus, when rotating in a gravity field.

2. GOVERNING EQUATIONS

The governing equations for the present problem may be expressed in either of two coordinate systems, one being fixed to the external gravity vector $\mathbf{g}$ and the other one to the rotating porous matrix. These two situations are depicted in Figs. 1(a) and (b), respectively. Strictly speaking, only the gravitationally-locked coordinate system of Fig. 1(a) may be termed 'inertial'. However, all solutions considered in this study are limited to weak angular velocities Ω', such that results for the coordinate system in Fig. 1(b) also correspond to an inertial reference frame.

In addition, it is assumed that the steady state form of Darcy's law prevails for all cases considered; that is, the filtration velocity adjusts itself instantaneously to the applied buoyancy forces. As a consequence, the time-dependent effects of rotation are felt only through the thermal inertia of the fluid-saturated porous matrix. At low angular velocities Ω', a set of equations based on either of the two coordinate systems may be used with equal success in the numerical approach; one set leads to a steady state solution whereas the other one is time-dependent. Results from both approaches, properly transformed, are identical.

The flow will be assumed to be two-dimensional. According to ref. [4], in the absence of rotation, this assumption is valid for a sufficiently short annulus. It is also valid for a long annulus, provided the Rayleigh number is sufficiently low. Also, from ref. [4], at higher Rayleigh numbers in a long annulus the flow is observed to remain two-dimensional over a large part of the annulus. Since we are interested in the perturbing effect of weak rotation, and the Rayleigh numbers are moderate, we will adopt the two-dimensional assumption.

2.1. *Rotating coordinate system*

Consider a horizontal porous annulus in steady rotation, with the coordinate frame rotating with the annulus. In such a coordinate frame the geometry is as shown in Fig. 1(b).

The momentum equation for flow in a rotating

† Permanent address: Department of Mechanical Engineering, Ecole Polytechnique (Campus de l'Universite de Montreal), C.P. 6079 Succursale A, Montreal, Québec, Canada H3C 3A7.

NOMENCLATURE

Da	Darcy number, equation (3a)
Ek	porous medium Ekman number, equation (3b)
Fr	Froude number, equation (3c)
g	gravitational acceleration [m s^{-2}]
K	permeability of the porous medium [m^2]
k	thermal conductivity of the saturated porous medium [W m^{-1} K^{-1}]
P	dimensionless pressure
p	dimensionless reduced pressure
r	dimensionless radial coordinate
R	radius ratio, equation (15)
Ra	Rayleigh number, equation (14a)
t	dimensionless time
T	dimensionless temperature difference, equation (14b)
ΔT_0	characteristic temperature difference, $(T_2' - T_1')$ [K]
u	dimensionless velocity in r-direction
v	dimensionless velocity in θ-direction.

Greek symbols

α	thermal diffusivity of the saturated porous medium, $(k/(\rho c)_f)$ [m^2 s^{-1}]
β	thermal expansion coefficient of the fluid [K^{-1}]
ε	porosity
θ	angular (i.e. circumferential) coordinate
θ_p	phase angle
μ	dynamic viscosity of the fluid [kg m^{-1} s^{-1}]
ν	kinematic viscosity of the fluid [m^2 s^{-1}]
ρ	density of the fluid [kg m^{-3}]
$(\rho c)_f$	heat capacity of the fluid [J m^{-3} K^{-1}]
$(\rho c)_p$	heat capacity of the saturated porous medium [J m^{-3} K^{-1}]
$(\rho c)_s$	heat capacity of the solid [J m^{-3} K^{-1}]
σ	heat capacity ratio, $(\rho c)_p/(\rho c)_f$
ϕ	dimensionless heat transfer rate averaged over the inner boundary
ψ	dimensionless stream function
Ω	dimensionless angular velocity, equation (14c)

Superscripts

$'$	dimensional variable
$*$	solid body rotation
$\bar{}$	variables in rotating coordinate frame, equation (28).

Subscripts

1	value on inner cylinder
2	value on outer cylinder
f	fluid velocity, equation (1).

porous medium may be derived from the Navier–Stokes equation for a continuum fluid [5]

$$\frac{\partial \mathbf{v}_f'}{\partial t'} + (\mathbf{v}_f' \cdot \nabla)\mathbf{v}_f' = -\frac{1}{\rho}\nabla P' + \nu \nabla^2 \mathbf{v}_f' + \mathbf{g}(t') - \boldsymbol{\Omega}' \times (\boldsymbol{\Omega}' \times \mathbf{r}') - 2\boldsymbol{\Omega}' \times \mathbf{v}_f'. \quad (1)$$

This equation is expressed in a coordinate frame rotating at a constant angular velocity $\boldsymbol{\Omega}'$; the fluid velocity vector is $\mathbf{v}_f'$. The last two terms on the right-hand side are the centrifugal force and Coriolis terms, respectively. A positive value of $\boldsymbol{\Omega}'$ corresponds to a coordinate frame rotating counterclockwise with respect to a fixed external reference frame. For the geometry of Fig. 1(b), the gravity vector is assumed to be fixed in the external reference frame; thus, when viewed from the coordinate frame rotating with the horizontal annulus, the gravity vector rotates clockwise at an angular speed Ω'.

By volumetric averaging of (1) and by neglecting the local and convective acceleration terms on the left-hand side [6, 7], the following momentum equation for flow in a porous medium results:

$$\frac{\mu}{K}\mathbf{v}' - \frac{\mu}{\varepsilon}\nabla^2 \mathbf{v}' = -\nabla P' + \rho \mathbf{g}(t') - \rho \boldsymbol{\Omega}' \times (\boldsymbol{\Omega}' \times \mathbf{r}') - 2\frac{\rho}{\varepsilon}\boldsymbol{\Omega}' \times \mathbf{v}' \quad (2)$$

where $\mathbf{v}'$ is the filtration velocity and K the permeability. The first and second terms on the left-hand side of (2) are the Darcy and Brinkman terms, respectively. The latter accounts for the viscous effects of the boundaries. In the rotating coordinate frame, the body force terms include the time-dependent external gravity field, $\mathbf{g}(t')$, the centrifugal acceleration term, and the Coriolis term, volumetric averaging being straightforward for this last term since Ω' is uniform throughout the medium.

The ratio of the Darcy and Brinkman terms is called the Darcy number

$$Da = K/L'^2 \quad (3a)$$

with L' being a characteristic length. The ratio of the Darcy term, which expresses the viscous resistance of the solid matrix, to the Coriolis term produces a porous medium Ekman number

$$Ek = \nu/K\Omega'. \quad (3b)$$

Further, the ratio of the third and second terms on the right-hand side of (2) represents the centrifugal/gravity force ratio in the form of a Froude number

$$Fr = \Omega'^2 r'/g. \quad (3c)$$

In the present paper we will assume the angular

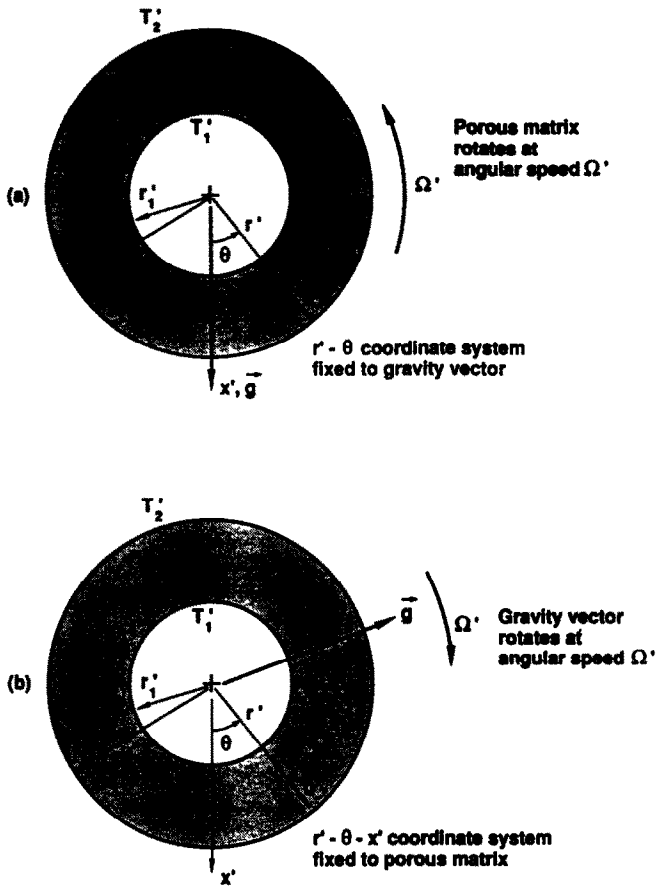

FIG. 1. Flow geometry and coordinate systems. (a) Non-rotating coordinate system: coordinates r'–θ fixed to the external gravity vector. The porous matrix rotates counterclockwise. (b) Rotating coordinate system: coordinates r'–θ fixed to the rotating porous matrix. Gravity vector rotates clockwise.

speed Ω' to be small, such that rotational effects may be neglected relative to the viscous resistance and the gravity field (i.e. we assume large Ek and small Fr). This is justified for certain food processing problems. For example, for a porous medium consisting of spheres of diameter 2 mm, and saturated with water, we have, approximately, $K = 4 \times 10^{-9}$ m^2 and $\nu = 1 \times 10^{-6}$ m^2 s^{-1}. If the annulus has an outer diameter of about 6 cm or less, and the rotation rate is restricted to 4 rad s^{-1} or less, the associated Ek and Fr ranges are $Ek > 60$ and $Fr < 0.1$.

With the practical values assumed above, we have $Da \approx 10^{-6}$. Consequently, the Brinkman term is expected to have a negligible effect on the results [8] and will not be considered.

With the neglect of rotational and boundary viscous effects in (2), and with the use of the Boussinesq approximation ($\Delta\rho \ll \rho$) and the linear relationship between density and temperature given by

$$\frac{\Delta\rho}{\rho} = -\beta\Delta T \tag{4}$$

the Darcy equations for flow in a porous medium, expressed in the two-dimensional polar coordinates of Fig. 1(b), are:

r-direction

$$u' = -\frac{Kg\beta}{\nu}(T' - T'_1)\cos(\Omega' t' + \theta) - \frac{K}{\mu}\frac{\partial p'}{\partial r'}; \tag{5a}$$

θ-direction

$$v' = \frac{Kg\beta}{\nu}(T' - T'_1)\sin(\Omega' t' + \theta) - \frac{K}{\mu}\frac{1}{r'}\frac{\partial p'}{\partial \theta} \tag{5b}$$

where p' is the reduced pressure (obtained by subtracting the hydrostatic component). The Darcy equations are time-dependent via the rotating gravity vector and the time dependence of T' and p'.

The other governing equations are the continuity equation

$$\frac{1}{r'}\left(\frac{\partial r' u'}{\partial r'} + \frac{\partial v'}{\partial \theta}\right) = 0 \tag{6}$$

and the energy equation

$$(\rho c)_p \frac{\partial T'}{\partial t'} + (\rho c)_f \left(u' \frac{\partial T'}{\partial r'} + \frac{v'}{r'} \frac{\partial T'}{\partial \theta} \right) = k \nabla^2 T' \quad (7)$$

where

$$(\rho c)_p = \varepsilon (\rho c)_f + (1-\varepsilon)(\rho c)_s \quad (8)$$

and $(\rho c)_f$ is the heat capacity of fluid, $(\rho c)_s$ the heat capacity of solid, $(\rho c)_p$ the heat capacity of saturated porous medium, ε the porosity, and k the thermal conductivity of saturated porous medium.

The boundary conditions associated with equations (5)–(7) are

$$r' = r_1': \quad u' = 0, \quad T' = T_1'$$
$$r' = r_2': \quad u' = 0, \quad T' = T_2' > T_1'. \quad (9)$$

Equations (5)–(7) are made dimensionless by the use of the following reference scales:

characteristic length	r_1'
characteristic time	$(\rho c)_p r_1'^2/k = \sigma r_1'^2/\alpha$
characteristic velocity	$\dfrac{k}{(\rho c)_f r_1'} = \alpha / r_1'$
characteristic pressure	$\dfrac{k\mu}{(\rho c)_f K} = \alpha \mu / K$
characteristic temperature	$\Delta T_0 = T_2' - T_1'$ (10a–e)

with $\sigma = (\rho c)_p/(\rho c)_f$ and $\alpha = k/(\rho c)_f$.

In dimensionless form, the governing equations (5)–(7) become

$$u = -Ra\, T \cos(\Omega t + \theta) - \frac{\partial p}{\partial r} \quad (11a)$$

$$v = Ra\, T \sin(\Omega t + \theta) - \frac{1}{r} \frac{\partial p}{\partial \theta} \quad (11b)$$

$$\frac{1}{r} \left(\frac{\partial ru}{\partial r} + \frac{\partial v}{\partial \theta} \right) = 0 \quad (12)$$

$$\frac{\partial T}{\partial t} + u \frac{\partial T}{\partial r} + \frac{v}{r} \frac{\partial T}{\partial \theta} = \nabla^2 T \quad (13)$$

in which

$$Ra = Kg\beta \Delta T_0 r_1'/\nu\alpha$$
$$T = (T' - T_1')/\Delta T_0$$
$$\Omega = \Omega' \sigma r_1'^2/\alpha \quad (14a–c)$$

with boundary conditions

$$r = 1: \quad u = 0, \quad T = 0$$
$$r = r_2'/r_1' = R: \quad u = 0, \quad T = 1. \quad (15)$$

The parameters which appear are the Rayleigh number, Ra, the dimensionless rotation rate, Ω, and the radius ratio, R.

Pressure may be eliminated from equations (11a) and (11b) by cross-differentiation. We obtain

$$\nabla^2 \psi = -Ra \left[\sin(\Omega t + \theta) \frac{\partial T}{\partial r} + \frac{\cos(\Omega t + \theta)}{r} \frac{\partial T}{\partial \theta} \right] \quad (16)$$

where ψ is the stream function related to the velocity components by

$$u = \frac{1}{r} \frac{\partial \psi}{\partial \theta}; \quad v = -\frac{\partial \psi}{\partial r}. \quad (17a,b)$$

The rotation, combined with gravity, does not permit any assumption of symmetry (either centrosymmetry or symmetry with respect to a given diameter). Therefore, the boundaries at $r = 1$ and R cannot be connected by any streamline. In fact, one must allow for the possibility of a net circulating flow between the two boundaries. It follows that the appropriate boundary conditions for ψ and T are

$$r = 1: \quad \psi = \psi_1, \quad T = 0$$
$$r = R: \quad \psi = 0, \quad T = 1 \quad (18)$$

with ψ_1 corresponding to an unknown net circulating flow around the annulus.

An additional condition is required to find ψ_1. It may be obtained by using the periodicity condition [9]

$$\xi(r, \theta, t) = \xi(r, \theta + 2\pi, t) \quad (19)$$

where ξ stands for any physical variable, and by integrating equation (11b) first over $0 \leqslant \theta \leqslant 2\pi$ and, after substituting equation (17b), over $1 \leqslant r \leqslant R$, we obtain

$$\psi_1 = \frac{Ra}{2\pi} \int_1^R \int_0^{2\pi} T \sin(\Omega t + \theta)\, d\theta\, dr. \quad (20)$$

This equality relates the volume circulation around the annulus, ψ_1, to an integral of the circumferential buoyancy force.

Equations (13), (16) and (17), together with boundary conditions (18) and (20), describe the flow in a coordinate system rotating with the porous annulus. The governing parameters are Ra, Ω and R. The equations admit steady periodic solutions in which the flow and temperature fields rotate at a constant angular velocity within the annulus while being locked to the rotating external gravity vector.

2.2. *Non-rotating coordinate system*

Consider next a porous annulus which is in steady rotation with respect to a fixed (inertial) reference frame, as in Fig. 1(a). With respect to the fixed frame (in this case fixed to the gravity vector), the annulus rotates counterclockwise at a steady angular speed Ω'. For rectilinear motion of a porous medium without acceleration, Darcy's law remains the same as if the porous medium was at rest, except that a relative velocity appears [10]. In general, in a fluid body undergoing rotation each fluid particle experiences centrifugal and Coriolis forces. However, such forces

may be neglected at low rotation rates, as is assumed in the present study (i.e. large Ek and small Fr). Thus, the appropriate Darcy equations are, after accounting for the relative velocity:

r-direction

$$u' = \frac{K}{\mu}\left[-\rho g\beta(T'-T'_1)\cos\theta - \frac{\partial p'}{\partial r'}\right]; \quad (21a)$$

θ-direction

$$v'-\Omega' r' = \frac{K}{\mu}\left[-\rho g\beta(T'-T'_1)\sin\theta - \frac{1}{r'}\frac{\partial p'}{\partial \theta}\right]. \quad (21b)$$

Note that the time variable arises via the time dependence of T' and p'. If the latter are time invariant in the fixed frame, the velocity field is also time invariant.

The continuity equation is unchanged from its form in equation (6). However, the energy equation introduces an additional term because the motion of the porous matrix contributes to heat transport in the θ-direction. The energy equation becomes

$$(\rho c)_p\frac{\partial T'}{\partial t'} + (\rho c)_f\left[u'\frac{\partial T'}{\partial r'} + \frac{v'}{r'}\frac{\partial T'}{\partial \theta}\right] + [(\rho c)_p - (\rho c)_f]\Omega'\frac{\partial T'}{\partial \theta} = k\nabla^2 T'. \quad (22)$$

Using the characteristic quantities given in equation (10), and introducing the stream function, the governing dimensionless equations are

$$\frac{\partial T}{\partial t} + u\frac{\partial T}{\partial r} + \frac{v}{r}\frac{\partial T}{\partial \theta} - \left(\frac{1}{\sigma}-1\right)\Omega\frac{\partial T}{\partial \theta} = \nabla^2 T \quad (23)$$

$$\nabla^2\psi = -2\Omega/\sigma - Ra\left[\sin\theta\frac{\partial T}{\partial r} + \frac{\cos\theta}{r}\frac{\partial T}{\partial \theta}\right] \quad (24)$$

and

$$u = \frac{1}{r}\frac{\partial \psi}{\partial \theta}, \quad v = -\frac{\partial \psi}{\partial r} \quad (25a,b)$$

with boundary conditions

$$r = 1: \quad \psi = \psi_1, \quad T = 0$$
$$r = R: \quad \psi = 0, \quad T = 1. \quad (26)$$

The additional boundary condition needed to determine ψ_1, analogous to equation (20), is

$$\psi_1 = \Omega(R^2-1)/2\sigma + \frac{Ra}{2\pi}\int_1^R\int_0^{2\pi} T\sin\theta\,d\theta\,dr. \quad (27)$$

Note in the above set of equations (23)–(27) that the time variable enters explicitly only in the energy equation. Indeed, as we shall see later for the present non-rotating, gravitationally-fixed coordinate system, steady state solutions arise. Also note that four parameters appear in the governing equations: Ra, Ω, R and the heat capacity ratio σ.

2.3. *Conversion between rotating and non-rotating reference frames*

Solutions of the governing equations are readily transferred between the rotating and the non-rotating, gravitationally-locked, coordinate frames. All physical quantities, except v, ψ, and θ, exactly correspond in the two systems. To avoid confusion, we will henceforth attach overbars to values from the rotating coordinate system, such that

$$v = \bar{v} + \Omega r/\sigma \quad (28a)$$

$$\psi = \bar{\psi} - \Omega(r^2 - R^2)/2\sigma. \quad (28b)$$

Quantities without overbars on the left refer to the *non-rotating* coordinate system of Fig. 1(a); such solutions are obtained from equations (23) to (27). Quantities with overbars refer to the *rotating* coordinate system of Fig. 1(b); such flows are governed by equations (13), (16)–(18), and (20).

3. NUMERICAL METHOD

Finite difference techniques with uniform mesh size (18×36) or (36×72) are used in the numerical approach to discretize the entire annulus. The Poisson equations (16) or (24) are solved by the method of successive over-relaxation. The energy equations (13) or (23) are solved by an alternating direction implicit method (ADI). Central differences are used in the numerical formulation of the advective terms.

The ADI method requires boundary conditions in r as well as θ. The only physical condition that prevails at the end points in the θ-direction is the periodicity condition (19). The resulting matrices are handled by a partition procedure, as used in ref. [11].

The value of the stream function on the inner boundary is found by numerically evaluating the integrals in equation (20) or (27) by using a type of trapezoidal rule integration.

Numerical computations were carried out with time increments ranging from 0.0005 to 0.002 until the flow and temperature fields reached the steady (or steady-periodic) state. The choice of initial conditions was not observed to have any effect on the final solution for the ranges of Ra and Ω considered.

4. RESULTS AND DISCUSSION

Results are presented for a range of Rayleigh numbers from $Ra = 50$ to 200, and for rotation rates from $\Omega = 0$ to 100π. The radius ratio was held fixed at $R = 2$. Except for Fig. 5, the heat capacity ratio was taken as $\sigma = 1$.

The graphs shown in Fig. 2 are temperature and flow fields obtained by increasing the rotation rate, Ω. The left column displays isotherms, the center column displays steady-state streamlines (ψ) in the gravitational reference frame (i.e. Fig. 1(a)), and the right

column displays streamlines ($\bar{\psi}$) relative to the rotating porous matrix. Note for Fig. 2(a), when $\Omega = 0$, that the two flow fields are identical and $\psi = \bar{\psi}$. In the rotating coordinate frame (i.e. Fig. 1(b)), the flows are steady periodic and are locked with the rotating gravity vector. For convenience, the flows in this coordinate frame are shown with the gravity vector in the downward position. On each of the graphs in Fig. 2, the positive θ-direction is in the counterclockwise direction. Figure 2(a), with $\Omega = 0$, reproduces the results published by Caltagirone [4]. Also shown in Fig. 2 are the heat transfer rates ϕ_1 and ϕ_2 on the inner and outer boundaries, respectively. These values are in the ratio $\phi_1/\phi_2 = 2$ when the radius ratio $R = 2$.

The graphs of Fig. 2 were obtained by numerically solving equations (23) and (24) in the gravitational reference frame. The flow field relative to the porous matrix, $\bar{\psi}$, was deduced by using equation (28b).

A solution obtained by solving equations (13) and (16) in the rotating reference frame produces results which are, except for the angular position of the gravity vector, identical to Fig. 2(d). The temperature and flow fields T and $\bar{\psi}$ are steady periodic and rotate at a constant angular speed Ω. Except for the angular position, the temperature and flow fields in Fig. 2 can be obtained from equations (13) and (16).

From the sequence of Fig. 2, we may notice some of the effects induced by rotation, namely the loss of symmetry, the occurrence of a net circulating flow $\bar{\psi}_1$, and the appearance of a phase angle (defined as θ_p) between the gravity direction and the location of the maximum local heat transfer on the outer boundary. Another important effect is the drastic reduction in the overall heat transfer between the outer and inner radial boundaries with increasing Ω.

Figure 3 displays θ_p, ϕ_1, $\bar{\psi}_1$, and $\Delta\bar{\psi}_{max}$ as functions of the rotation rate Ω for $Ra = 100$ and $\sigma = 1$. $\Delta\bar{\psi}_{max} = (\bar{\psi}_{max} - \bar{\psi}_{min})/2$ is a measure of the intensity of the flow relative to the porous matrix. Results for other values of Ra are shown in Fig. 4.

4.1. *Effect of rotation on heat transfer*

It is observed in Figs. 3 and 4(a) that the heat transfer rate decreases monotonically towards the

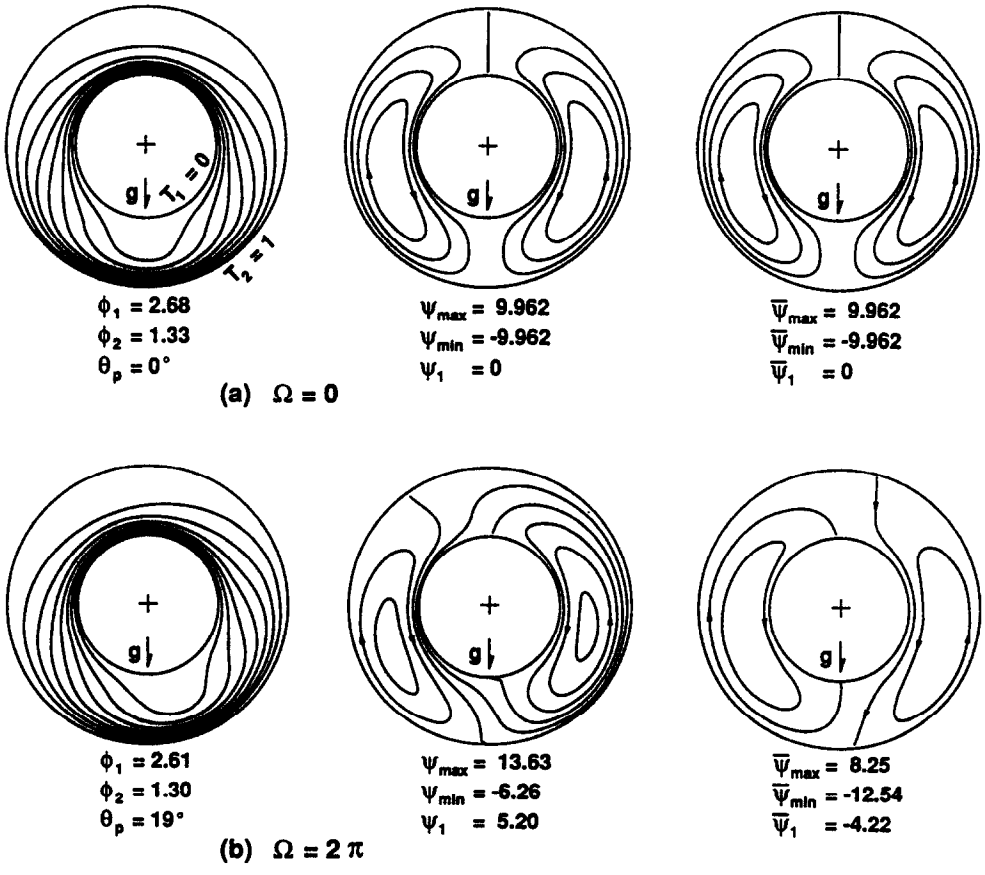

FIG. 2. Isotherms (left column), streamlines ψ (center column), and streamlines $\bar{\psi}$ (right column) for a range of rotation rates, Ω, with $Ra = 100$ and $\sigma = 1$. The center column of ψ-streamline graphs corresponds to a coordinate system fixed to the gravity vector; the porous annulus rotates counterclockwise. The right column of $\bar{\psi}$-streamline graphs shows streamlines relative to the porous matrix; the coordinate system rotates with the matrix, the gravity vector rotates clockwise, and the flow is shown when g is directed downwards.

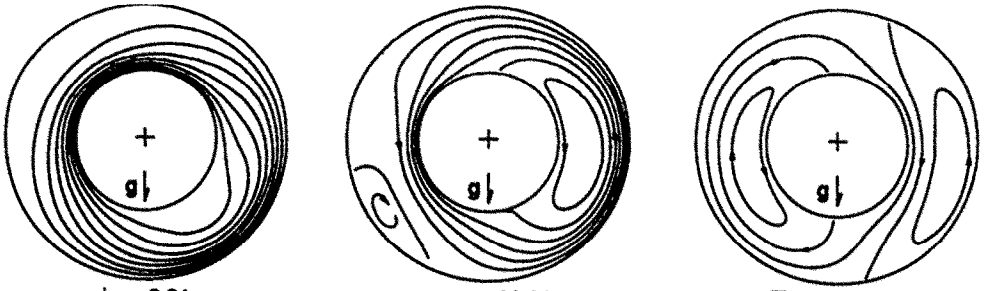

(c) $\Omega = 5\pi$

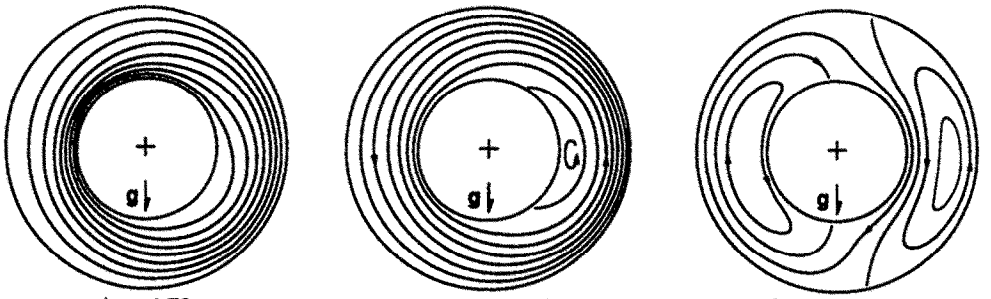

(d) $\Omega = 10\pi$

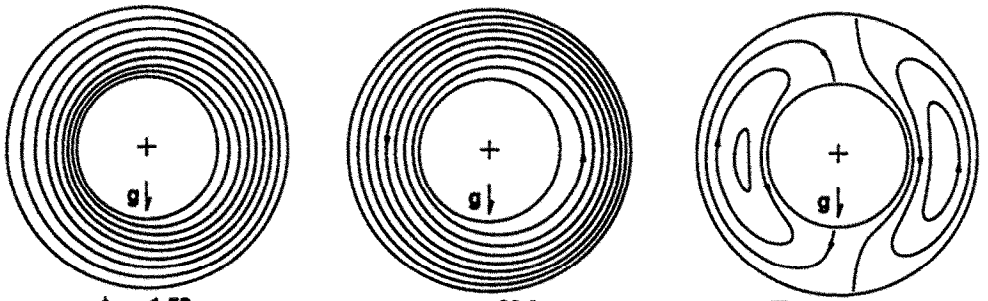

(e) $\Omega = 20\pi$

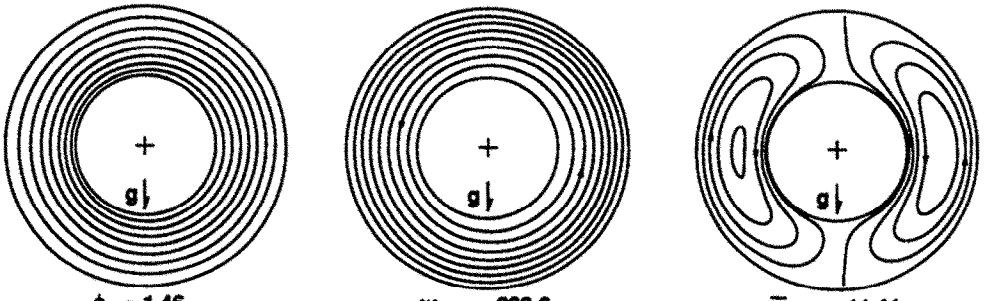

(f) $\Omega = 50\pi$

FIG. 2—*Continued.*

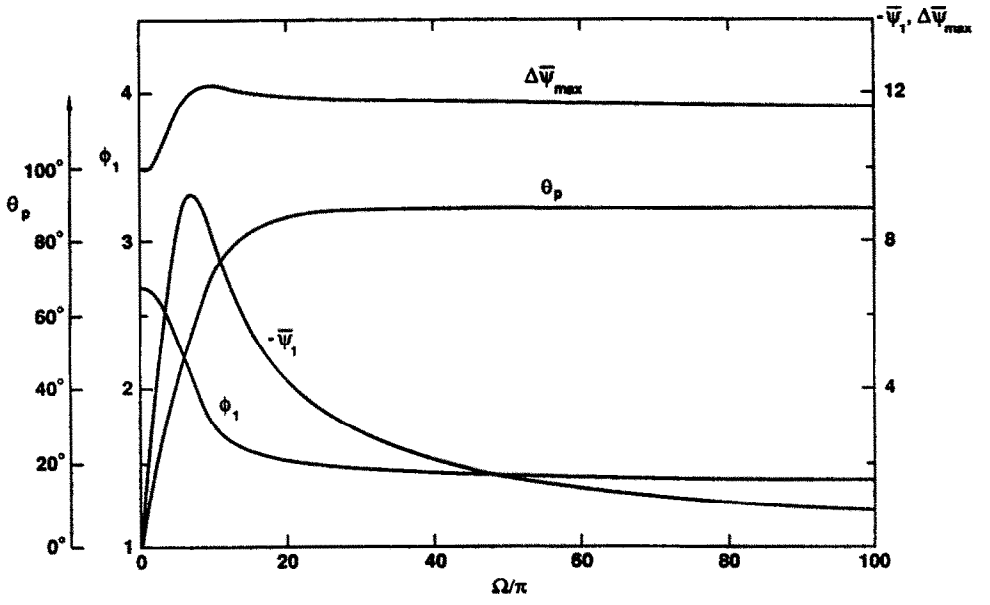

FIG. 3. Effect of angular velocity Ω on the phase angle, θ_p, the heat transfer rate at the inner boundary, ϕ_1, the net circulation around the annulus, $\bar{\psi}_1$, and the flow intensity relative to the porous matrix, $\Delta\bar{\psi}_{max} = (\bar{\psi}_{max} - \bar{\psi}_{min})/2$. $Ra = 100$ and $\sigma = 1$.

pure conduction value of 1.44 as Ω is increased. It is also observed in Fig. 3 that the intensity of the flow field relative to the porous matrix, which may be expressed as $\Delta\bar{\psi}_{max}$, increases slightly and remains quite strong for all Ω. This apparent contradiction disappears when one considers that the orientation of the flow field $\bar{\psi}$ shown in Figs. 2(b)–(f) (i.e. the right-hand column of graphs) is locked with the gravity vector and rotates continuously with time. In other words, the streamlines shown do not correspond to a steady state and consequently do not represent fluid trajectories.

A way to understand physically how the convective heat transfer is reduced with increasing Ω is to consider the sequence of flow fields ψ in Fig. 2 (i.e. the center column of graphs). These flow fields correspond to steady states and consequently the streamlines shown describe the paths of fluid particles around the annulus. The heat transport from outer to inner boundary is related to the amplitude of the fluid motion in the radial direction and it is observed in these figures that this amplitude is reduced with increasing Ω.

The presence of the Brinkman term in the governing equations would not change the qualitative behavior already described. As shown in ref. [7], an increasing Darcy number would lower the heat transfer rates given in Figs. 3 and 4(a).

The intensity of the flow field relative to the porous matrix, $\Delta\bar{\psi}_{max}$, is higher with rotation than without rotation. This is understandable when the following facts are considered: the gravity field $\mathbf{g}$ is always present with the same strength, no matter how high the value of Ω; there is no fluid inertia and the fluid particles are immediately accelerated to the velocity that equilibrates with the imposed buoyancy force; and the temperature field associated with the reduced convective heat transfer does not exert on the flow field $\bar{\psi}$ the buoyant force that occurs when Ω is equal to zero.

The heat transfer reduction is accompanied by the phase angle θ_p defined previously. As seen in Figs. 3 and 4(c), θ_p increases from zero to an asymptotic value of $\pi/2$ with increasing Ω. Also, the net circulating flow $\bar{\psi}_1$ destroys the symmetry of the flow observed in Fig. 2(a). From Figs. 3 and 4(b), $\bar{\psi}_1$ increases, reaches a maximum, and then decreases as Ω is increased. In the latter limit, there is a tendency for the original symmetry to reappear.

It may be noticed in Figs. 3 and 4 that the quantities θ_p, ϕ_1, $\bar{\psi}_1$ and $\Delta\bar{\psi}_{max}$ satisfy the following conditions of symmetry and antisymmetry in the neighborhood of $\Omega = 0$ as required by the physics of the problem:

$$\theta_p(\Omega) = -\theta_p(-\Omega), \qquad \phi_1(\Omega) = \phi_1(-\Omega)$$
$$\bar{\psi}_1(\Omega) = -\bar{\psi}_1(-\Omega), \quad \Delta\bar{\psi}_{max}(\Omega) = \Delta\bar{\psi}_{max}(-\Omega).$$

In summary, the effect of an imposed rotation is to disturb the flow pattern in a way that greatly reduces the convective heat transfer. This is the major consequence of rotation within the range of governing parameters considered here and a similar trend is expected for other problems involving rotation about a horizontal axis. A decrease of heat transfer by rotation has also been reported by Hide and Mason [12] for the case of a fluid-filled vertical annulus rotating about its axis. For that situation, however, the inner boundary was heated and heat transfer inhi-

bition occurs for different reasons, tied up to the axisymmetry of the flow.

4.2. *Induced net circulating flow*

Without convection, the net circulating flow, relative to the coordinate system fixed with the gravity vector, would be the one corresponding to solid body rotation, $\psi_1^* = \Omega(R^2-1)/2\sigma$. In other words, as shown in Fig. 4(b), the occurrence of a non-zero value for $\bar{\psi}_1$ ($\bar{\psi}_1 = \psi_1 - \psi_1^*$ from equation (28b)) is clearly the result of free convection. Without rotation, the free convection produces a flow field consisting of two contrarotating cells, as shown in Fig. 2(a). When a small rotation rate is introduced, the presence of those cells, which are locked with the gravity vector, constitutes an obstacle to the full establishment of solid

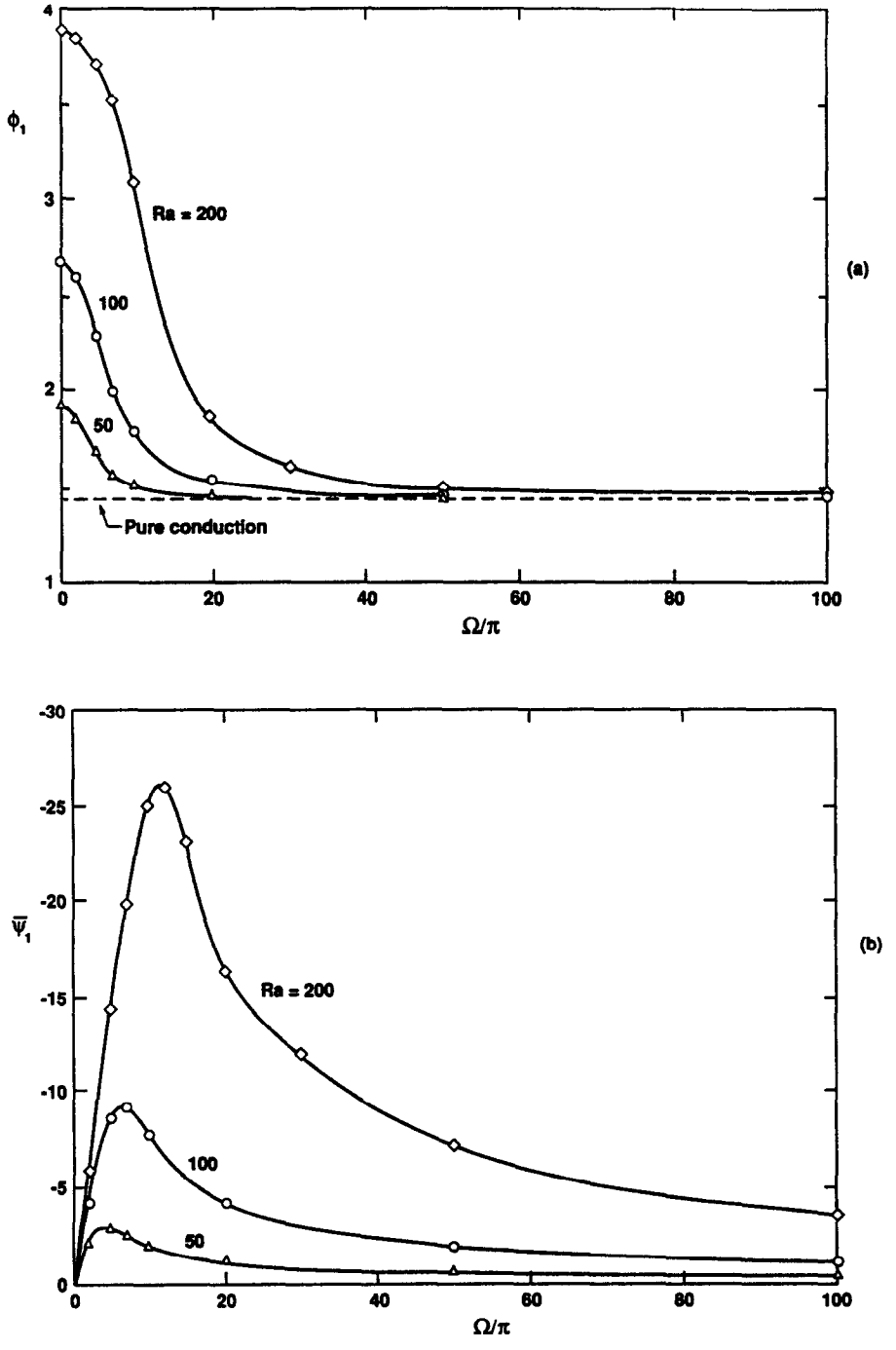

FIG. 4. Effect of Ra and Ω, $\sigma = 1$. (a) Heat transfer rate at inner boundary, ϕ_1. (b) Net circulation, $\bar{\psi}_1$, around the annulus. (c) Phase angle θ_p.

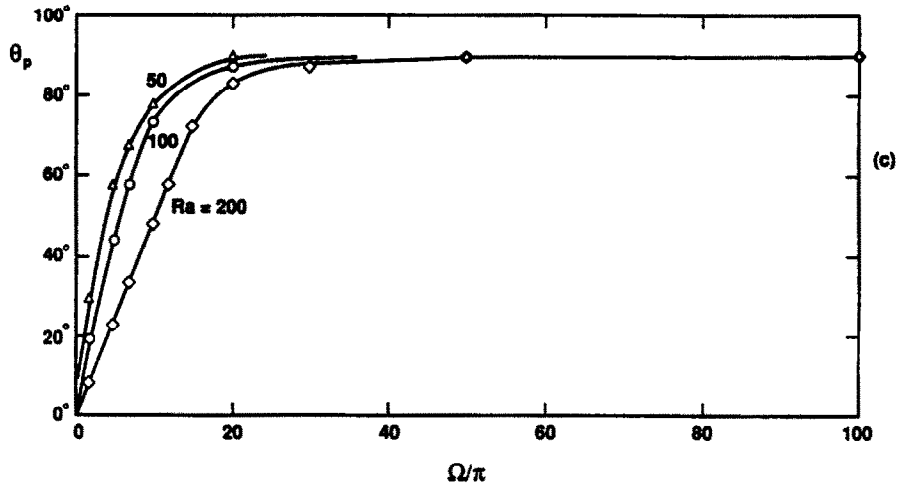

FIG. 4—*Continued.*

body rotation for the fluid. Thus ψ_1 is smaller than ψ_1^* and a negative value of $\bar{\psi}_1$ occurs. With increasing Ω, the cells gradually vanish from the flow field (sequence of ψ fields in Fig. 2) and $\psi_1 \to \psi_1^*$.

4.3. *Influence of* σ

The role of σ, which appears in equations (23), (24) and (27), arises from the connection between the rotational and gravitationally-locked coordinate systems expressed by the relationship $\psi = \bar{\psi} - \Omega(r^2 - R^2)/2\sigma$. This is evidenced by the results in Fig. 5 (which have been obtained from equations (23) and (24)), and which correspond to $\sigma = 0.5$. While the temperature field and the flow field $\bar{\psi}$ in the rotating frame correspond perfectly to Fig. 2(d), the flow field ψ in the gravitational frame is more comparable to Fig. 2(e). As the heat capacity $(\rho c)_f$ is larger in Fig. 5, a smaller amplitude of fluid motion in the radial direction is required to convey the same amount of heat between the two boundaries.

5. SUMMARY

Numerical calculations were carried out to study natural convection in a horizontal annular porous layer in rotation about its own axis in a gravity field. The outer boundary of the annulus was maintained at a higher temperature than the inner boundary. Flow fields were examined in both rotating and gravitationally-fixed coordinate frames. Rotational effects arise only through the thermal inertia of the porous matrix. Since fluid inertia effects do not arise in the Darcy momentum equations, the natural convection flows were observed to lock onto the rotating gravity vector.

Natural convection in the presence of rotation induces a net circulating flow around the annulus *relative* to the rotating matrix ($\bar{\psi}_1$ in Figs. 3 and 4(b)). Also, the intensity of natural convection within the annulus, relative to the rotating matrix, was observed to increase slightly with rotation rate ($\Delta\bar{\psi}_{max}$ in Fig.

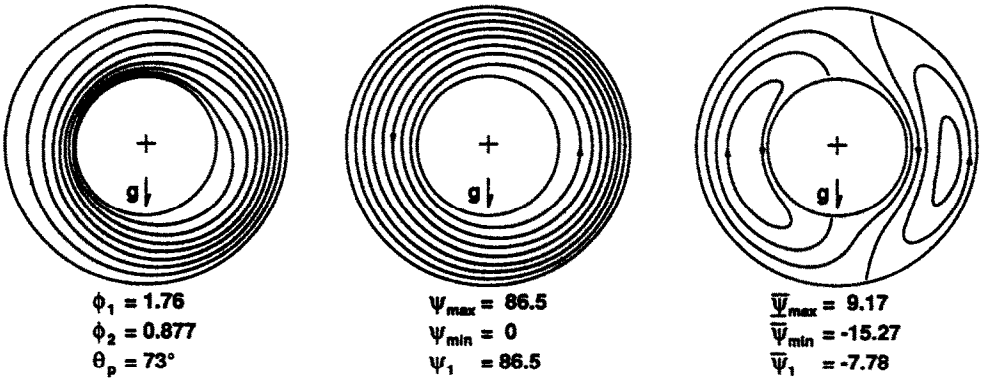

FIG. 5. Isotherms (left graph), streamlines ψ (center graph), and streamlines $\bar{\psi}$ (right graph) when $\Omega = 10\pi$, $Ra = 100$ and $\sigma = 0.5$. Compare with Fig. 2(d) to deduce the effect of σ.

3) with Ra constant. Most significantly, the convective heat transfer rate was observed to *decrease* with increasing rotation rate (the heat transfer rate, ϕ_1, at the inner boundary is shown in Figs. 3 and 4(a)). This is attributable to the heat capacity, and rotation, of the porous matrix. As the rotation rate, Ω, is increased, fluid trajectories relative to the gravitational frame (the ψ-fields in Fig. 2) show a reduced radial amplitude. This corresponds to a reduced radial convective heat transfer.

Acknowledgements—The authors wish to acknowledge the support of Ecole Polytechnique for a sabbatical leave (Luc Robillard) and the National Science Foundation for support under grant MEA 8401489. This research was conducted using the Cornell National Supercomputer Facility (CNSF), a resource of the Cornell Theory Center, which receives funding from NSF, IBM Corporation, New York State, and the Theory Center Corporate Research Institute. We also wish to acknowledge helpful discussions with Faluso Ladeinde, William R. C. Phillips, and Sidney Leibovich.

REFERENCES

1. C. O. Ball and F. C. W. Olson, *Sterilization in Food Technology*. McGraw-Hill, New York (1957).
2. L. E. Clifcorn, G. T. Peterson, J. M. Boyd and J. H. O'Neil, A new principle for agitating in processing of canned foods, *Fd Technol.* **4**, 450–460 (1950).
3. F. Ladeinde, Studies of thermal convection in self-gravitating and rotating horizontal cylinders in a vertical external gravity field, Ph.D. Thesis, Cornell University, Ithaca, New York (1988).
4. J. P. Caltagirone, Thermoconvective instabilities in a porous medium bounded by two concentric cylinders, *J. Fluid Mech.* **76**, 337–362 (1976).
5. G. K. Batchelor, *An Introduction to Fluid Dynamics*. Cambridge University Press, London (1967).
6. P. Cheng, Heat transfer in geothermal systems. In *Advances in Heat Transfer*, Vol. 14, pp. 1–105. Academic Press, New York (1978).
7. J. Bear, *Dynamics of Fluids in Porous Media*. Elsevier, New York (1972).
8. P. Vasseur and L. Robillard, The Brinkman model for boundary layer regime in a rectangular cavity with uniform heat flux from the side, *Int. J. Heat Mass Transfer* **30**, 717–727 (1987).
9. M. Prud'homme, L. Robillard and P. Vasseur, A study of laminar free convection in a non-uniformly heated annular fluid layer, *Int. J. Heat Mass Transfer* **30**, 1209–1222 (1987).
10. M. Prats, The effect of horizontal fluid flow on thermally induced convection currents in porous mediums, *J. Geophys. Res.* **71**, 4835–4838 (1966).
11. W. R. C. Phillips, The generalized lagrangian mean equations and streamwise vortices. In *Near Wall Turbulence* (Edited by S. Kline). Hemisphere, New York (1988).
12. R. Hide and P. J. Mason, Heat transfer in geothermal systems—sloping convection in a rotating fluid, *Adv. Phys.* **24**, 47–100 (1975).

INHIBITION DU TRANSFERT THERMIQUE CONVECTIF DANS UNE COUCHE POREUSE ANNULAIRE TOURNANT A FAIBLE VITESSE ANGULAIRE

Résumé—On étudie la convection naturelle dans une couche poreuse annulaire horizontale, en rotation autour de son axe. Des conditions aux limites isothermes sont appliquées sur les frontières intérieure et extérieure, cette dernière étant plus chaude. Aucune symétrie par rapport à un diamètre vertical ne peut être espéré pour les champs de température et de vitesse et on doit considérer toute la région. On obtient numériquement des solutions permanentes bidimensionnelles. Les résultats montrent que la rotation génère un écoulement de circulation autour de l'anneau par rapport à la matrice poreuse et qu'elle réduit notablement le transfert thermique global. Ces effets se produisent à des vitesses angulaires relativement faibles pour lesquelles la force centrifuge est négligeable à celle de pesanteur et les effets d'inertie peuvent être négligés.

BEHINDERUNG DES KONVEKTIVEN WÄRMETRANSPORTS IN EINEM PORÖSEN, LANGSAM ROTIERENDEN RINGSPALT

Zusammenfassung—Die natürliche Konvektion in einem horizontalen porösen Ringspalt, der um seine Achse rotiert, wird untersucht. An der inneren und äußeren Berandung herrscht konstante Temperatur, wobei die äußere Berandung wärmer ist. Unter solchen Bedingungen kann nicht erwartet werden, daß das Strömungs- und das Temperaturfeld bezüglich der senkrechten Achse symmetrisch ist—der gesamte Ringraum muß betrachtet werden. Das zweidimensional stationäre Problem wird gelöst. Die Ergebnisse zeigen, daß die Rotationsbewegung eine Zirkulationsströmung im Ringraum verursacht, welche die poröse Matrix in Umfangsrichtung durchdringt und den Gesamtwärmeübergang drastisch beeinträchtigt. Diese Effekte treten bei relativ kleinen Winkelgeschwindigkeiten auf, bei denen die Zentrifugalkräfte gegenüber der Schwerkraft vernachlässigt werden können, dies gilt auch für die Trägheitseffekte.

ПОДАВЛЕНИЕ КОНВЕКТИВНОГО ТЕПЛОПЕРЕНОСА В КОЛЬЦЕВОМ ПОРИСТОМ СЛОЕ, ВРАЩАЮЩЕМСЯ СО СЛАБОЙ УГЛОВОЙ СКОРОСТЬЮ

Аннотация—Исследуется естественная конвекция в горизонтальном кольцевом пористом слое, вращающемся вокруг своей оси. На внутреннюю и внешнюю границы наложены изотермические граничные условия, причем внешняя граница нагрета сильнее. При данных условиях нельзя ожидать симметрии течения относительно вертикального диаметра, и следует рассматривать температурные поля во всей кольцевой области. Численно получены двумерные стационарные решения. Результаты показывают, что вращение способствует появлению результирующего циркуляционного течения вокруг кольца относительно пористой матрицы и значительно снижает суммарный теплоперенос. Данные эффекты наблюдаются при сравнительно низких значениях угловой скорости, для которых центробежные силы пренебрежимо малы по сравнению с силой тяжести, и инерционными эффектами можно пренебречь.